

Heterogeneous & Homogeneous & Bio- & Nano-

CHEMCATCHEM

CATALYSIS

Accepted Article

Title: Iron and cobalt corroles in solution and on carbon nanotubes as molecular photocatalysts for hydrogen production by water reduction

Authors: Miguel A. Morales Vásquez, Mariana Hamer, Nicolas I. Neuman, Alvaro Y. Tesio, Andrés Hunt, Horacio Bogo, Ernesto J. Calvo, and Fabio Doctorovich

This manuscript has been accepted after peer review and appears as an Accepted Article online prior to editing, proofing, and formal publication of the final Version of Record (VoR). This work is currently citable by using the Digital Object Identifier (DOI) given below. The VoR will be published online in Early View as soon as possible and may be different to this Accepted Article as a result of editing. Readers should obtain the VoR from the journal website shown below when it is published to ensure accuracy of information. The authors are responsible for the content of this Accepted Article.

To be cited as: *ChemCatChem* 10.1002/cctc.201700349

Link to VoR: <http://dx.doi.org/10.1002/cctc.201700349>

WILEY-VCH

www.chemcatchem.org



Iron and cobalt corroles in solution and on carbon nanotubes as molecular photocatalysts for hydrogen production by water reduction

Miguel A. Morales Vásquez^{[a]§}, Mariana Hamer^{[b]§}, Nicolás I. Neuman^{[a][c]}, Alvaro Y. Tesio^[a], Andrés Hunt^[a], Horacio Bogo^[a], Ernesto J. Calvo^[a] and Fabio Doctorovich^{[a]*}

^[a] INQUIMAE; Departamento de Química Inorgánica, Analítica y Química Física; CONICET; Facultad de Ciencias Exactas y Naturales; Universidad de Buenos Aires. Ciudad Universitaria; Pabellón II; Buenos Aires (C1428EHA); Argentina.

^[b] Instituto de Nanosistemas, Universidad Nacional de San Martín; CONICET, Buenos Aires (B1650); Argentina.

^[c] Departamento de Física, FBCB-UNL, CONICET, Facultad de Bioquímica y Ciencias Biológicas, Ciudad Universitaria, Ruta N 168 S/N, S3000ZAA Santa Fe, Argentina

§ These authors participated equally in the development of this work.

*e-mail: doctorovich@qi.fcen.uba.ar; Fax: 54-11-4576-3341

RECEIVED DATE

Abstract:

Here we report the use of cobalt and iron corrole complexes as catalysts of H₂O reduction to generate H₂. Electro and photocatalysis has been used in the case of dissolved corroles for water reduction with inspiring results. Carbon nanotubes doped with corroles were used as photo-electrochemical catalysts allowing getting very low overpotential values and increased hydrogen production, achieving incredibly high turnover numbers and turnover frequencies of ca. 10⁷ and 10⁵, respectively. Through this last process we were able to obtain 1mmol of H₂ by using minuscule amounts of catalyst, in the order of pictograms. The reactions can be carried out in water, without the need of organic solvents. Remarkably, the photoelectrochemical catalytic efficiency was increased by five orders of magnitude when adsorbing the molecular catalysts onto carbon nanotubes.

Introduction

Replacement of fossil fuels with renewable energy sources, such as solar or wind, requires energy storage for the periods where these are inactive.^[1] Hydrogen obtained from water is a candidate of great interest to replace these other sources of energy as it is a clean, cheap and renewable fuel.^[2] Many techniques for H₂ production from natural gasoline, methanol, gas, biomass, and other non-renewable materials have been studied,^[1] but the efficient generation from water still remains the crux of a hydrogen-based economy.^[3]

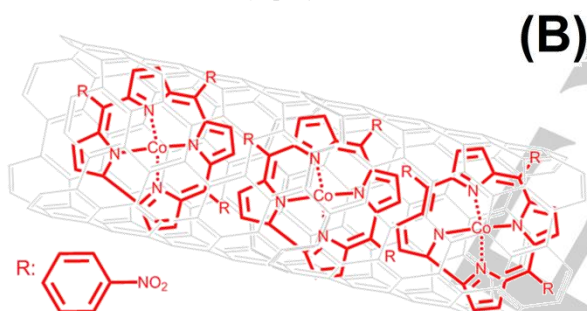
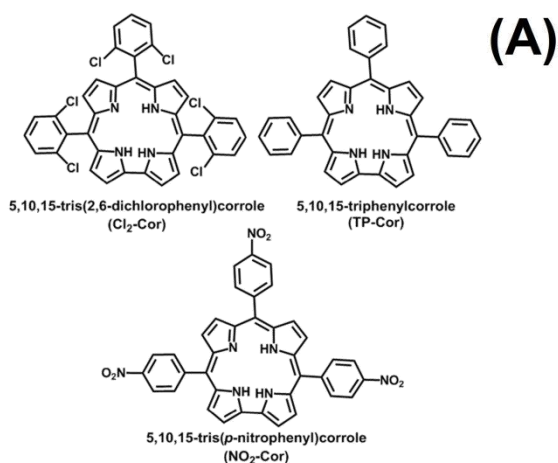
Metallocorroles and metalloporphyrins have shown to be promising potential catalysts for H₂ evolution in photocatalytic systems, in which a sensitizer mediates electron transfer from a sacrificial donor to the catalyst, which in turn reduces H⁺ to H₂.^[1] Corroles are 18- electron tetrapyrrolic macrocycles containing a direct pyrrole-pyrrole bond,^[2] and have a smaller cavity and lower symmetry-C_{2v} compared to porphyrins.^[3] Corroles have several interesting properties, among which is their trianionic nature upon deprotonation, which tend to stabilize transition metals in higher oxidation states compared with porphyrins.^[4-6] They also have a higher N-H acidity and high fluorescence levels.^[7-10]

Efficient synthetic methods developed by Gross *et al.*^[11,12], Paolesse *et al.*^[13] and Gryko *et al.*^[14,15] opened the doors for the progress of many new studies in corrole (photo and electro-) chemistry, spectroscopy and applications. Later Spiro *et al.*^[16] have shown Co^I porphyrin electrocatalyzed formation of H₂ in solution, and more recently we have reported hydrogen evolution using a cobalt porphyrin anchored on a gold electrode with a TON≈10⁶.^[17]

Due to the trianionic nature of free base corroles, the metal centers of corroles can reach oxidized states more easily than porphyrins. Therefore, the photoreduced Co^I corroles should be more reactive towards H⁺ reduction. This behavior was observed by Solomon *et al.*^[18] who studied the differences in energy in the oxidation state between corroles and porphyrins, and their interactions with metals. They

showed that there are more accessible states in the corrole which allows more accessible reduction of the metal center.

Hydrogen obtained in photocatalytic systems is produced by reduction of the catalyst using electrons obtained from a sacrificial donor; electron transfer occurs by way of a photoinduced sensitizer, which is regenerated by the sacrificial donor.^[4] However; photocatalysis has not been used in the case of corroles for water reduction.



Scheme 1. (A) Synthesized corroles. (B) Schematic representation of the absorbed metalcorrole on SWNT.

On the other hand, fundamental progress has been made in developing novel material structures for gaining this goal. Nanomaterial composites and structures, including inorganic, molecular and hybrid organic/inorganic materials,^[19,20] have been explored to meet specific requirements such as a light-absorbing wavelength modification,^[21,22] photoinduced charge separation^[23,24] and a faster water-splitting reaction.^[25] A great number of catalysts systems for energy storage and conversion has been based on carbon nanotubes (CNT) as they have the capability to contribute not only in charge injection and extraction, but also they increase the direct flow of photo-generated electrons.^[26-28] Recently, CNT were used in the synthesis of different

nanomaterials in order to improve the reduction of oxygen^[27,29,30], reduction of nitric oxide^[30] and oxidation of water.^[19,31]

In this work, we describe photocatalytic H₂ evolution experiments performed using cobalt and iron corroles (Scheme 1A) and discuss the relation between the catalyst efficiencies and their electrochemical and physicochemical properties. Furthermore, we describe the synthesis, characterization and photoreactivity of carbon nanotubes (MWNT) doped with Co(III)-Corrole (Scheme 1B) towards water reduction in aqueous solution.

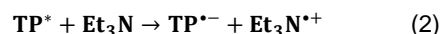
Results and Discussion

- Study of hydrogen production using corroles as photocatalysts.

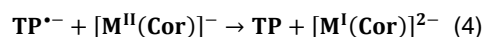
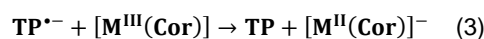
Free base corrole ligands were synthesized and in a second step were metallated with cobalt and iron. The main spectroscopic and electrochemical parameters of the obtained metalcomplexes are summarized in Table S1.

Experiments to determine the performance and the catalytic parameters for H₂ production for these organic catalysts in solution were performed using the setups shown in the Supporting Information (Figures S1-S4) using TEA (triethylamine) as sacrificial donor and TP (terphenyl) as a sensitizer.^[32]

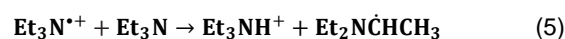
In 2002 Gross *et al.*^[33], reported a similar set up for catalytic reduction of CO₂, and described the following mechanism:

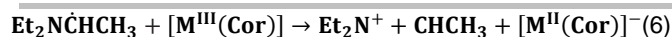


The metal center is readily reduced by the radical TP^{•-}, which has a very negative reduction potential (-2.45 V vs SCE in dimethylamine).^[34]



Et₃N^{•+} reacts with a molecule of TEA to form a carbon centered radical (E_{1/2}= -1.12 V vs. SCE in MeCN), which reduces the metal center [M^{III}(Cor)], but cannot reduce [M^{II}(Cor)]⁻.^[35]





The photochemical reduction causes the production of acid (as shown in reaction 7), which can protonate $[\text{M}^{\text{I}}(\text{Cor})]^{2-}$ and subsequently form the respective metal hydride, which can be protonated to form H_2 , or hydrogenate the macrocycle (as seen with porphyrins).^[32,35,36]



The addition of TEA did not result in a significant change in the UV-Vis spectra. However TEA may replace the axial ligand and also reduce the metal center.^[32,36,37] It is important to emphasize that no hydrogen is obtained under the present reaction conditions from TEA if the photocatalysis is carried out in the absence of water.

Hydrogen production was confirmed by detecting the produced gas while carrying out photocatalysis experiments, as the reaction system was connected to a DEMS (Figure S4). Figure S5(A) and (B) show the identification of the gas generated during the photocatalysis: hydrogen ($m/q = 2$); argon ($m/q = 40$) is used to obtain the inert atmosphere. Furthermore, while following the ionic current ($m/q=2$) in real time, the immediate intense bubbling (Figure S6 and multimedia) and formation of H_2 after the addition of H_2O to the catalyst/TP/TEA mixture can be observed.

Table 1 summarizes the results for H_2 generation for all the catalysts tested. The amount of H_2 produced by cobalt and iron metallocorroles is similar, with the latter being a little less efficient.

Table 1. Results of hydrogen production.^[a]

Catalyst	TON	TOF (min^{-1})	H_2 (mol) $\times 10^4$
$\text{NO}_2\text{-Cor-Co}$	113.3 ± 1.1	3.76 ± 0.12	8.5 ± 0.9
TP-Cor-Co	80.4 ± 0.9	1.79 ± 0.15	6.0 ± 1.1
$\text{Cl}_2\text{-Cor-Co}$	83.1 ± 1.1	3.30 ± 0.12	6.2 ± 0.9
$\text{NO}_2\text{-Cor-Fe}$	86.3 ± 1.2	1.9 ± 0.8	6.5 ± 0.8
TP-Cor-Fe	80.0 ± 1.1	1.8 ± 0.6	6.0 ± 1.2
$\text{Cl}_2\text{-Cor-Fe}$	83.3 ± 1.0	3.7 ± 0.9	6.2 ± 0.7

^[a] All experiments were performed in triplicate. The reactions were carried out at r.t and with continuous UV irradiation. 7.5×10^{-5} mol of catalyst in the presence of 3 mM of TP and 5% v/v of TEA were dissolved in 10 mL of 1,4-dioxane.

Figure 1 shows the UV-Vis spectrum changes for $\text{NO}_2\text{-Cor-Co}$ while irradiating. After irradiating for 15 minutes the reduction of the metal center to Co(I) is observed (blue). Then, following the addition of water, the catalyst returns to its oxidized state (green). However, after the second addition of water the metallocorrole was degraded (orange). The volume of gas generated was measured by using the setup

depicted in Figure S1. Figure S7 shows the gas production for two catalysts, $\text{NO}_2\text{-Cor-Co}$ and $\text{Cl}_2\text{-Cor-Co}$, after the first addition of water. Since free radicals are formed, it is also possible that these free radicals intervene in chain reactions which regenerate the radicales and produce H_2 . The electron donor is triethylamine, as described above. Regarding the catalyst, it is thought that the Soret band disappears due to unwanted hydrogenation of the macrocycle.

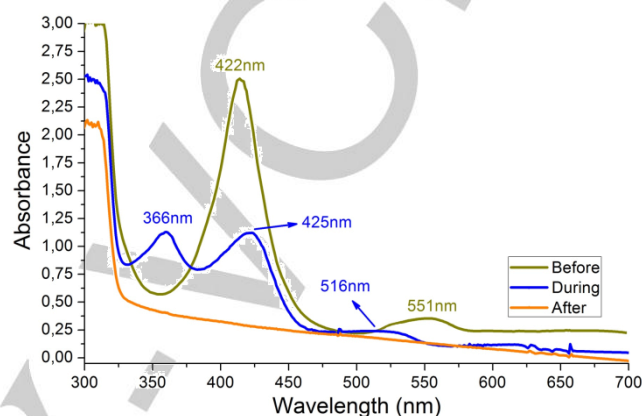


Figure 1. Time dependent traces taken from the UV-Vis spectrum using $\text{NO}_2\text{-Cor-Co}$ as photocatalyst. Green: before irradiation (Co(III)). Blue: during photocatalysis (Co(I)). Orange: degraded catalyst.

The different metallocorroles show similar values for TON, TOF and amount of H_2 generated (Table 1). This fact can be explained by the use of TP as a sensitizer, which having a very negative reduction potential is able to reduce all studied metallocorroles at similar rates, regardless of their individual redox properties. Furthermore, the TOF values are similar for most studied cobalt corroles, which suggests that the observed TOF is not a measure of the intrinsic efficiency of the metallocorrole, but a global TOF of the whole electron donor-photosensitizer-catalyst assembly. Therefore, we conducted several experiments where no TP was used in order to observe differences in the production of H_2 depending on the electron donating or withdrawing substituents. Some of the catalytic parameters obtained in the absence of TP are shown in Figure 2 and Table 2. The presence of an electron-attracting group such as $-\text{NO}_2$ increases the performance of the catalyst.

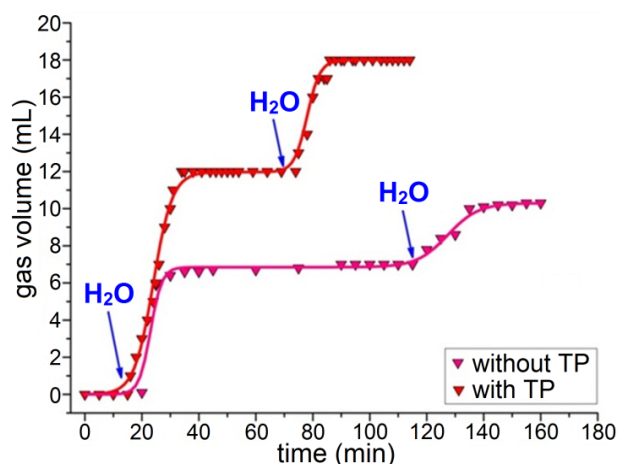


Figure 2. Evolution of gas formed during catalysis using $\text{NO}_2\text{-Cor-Co}$ catalyst in the presence and absence of TP and successive $100\ \mu\text{L}$ H_2O additions. Catalyst amount: 7.5×10^{-6} mol Temperature: $25\ ^\circ\text{C}$. TEA: 5% v/v; TP: 3 mM

Catalyst	TON	TOF (min^{-1})	H_2 (mol) $\times 10^{-4}$
$\text{NO}_2\text{-Cor-Co}$	76.3 ± 1.2	1.3 ± 0.4	5.7 ± 0.9
TP-Cor-Co	30.0 ± 1.1	0.5 ± 0.1	2.3 ± 0.8
$\text{Cl}_2\text{-Cor-Co}$	27.7 ± 1.0	0.5 ± 0.2	2.1 ± 0.9

^[a] All experiments were performed in triplicate. The reactions were carried out at r.t and with continuous UV irradiation. 7.5×10^{-6} mol of catalyst in the presence of 3 mM of TP and 5% v/v of TEA were dissolved in 10 mL of 1,4-dioxane.

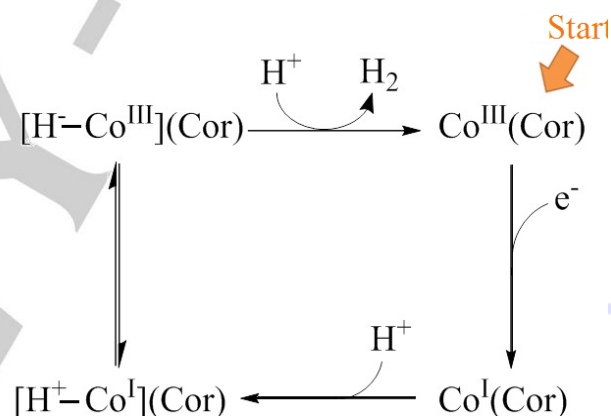
There appears to be a correlation between the absorptivities of the LMCT bands in the 200-300 nm range for all cobalt corroles and the efficiency of H_2 production in the absence of a second photosensitizer (TP). Since the lamp used in the experiments has excitation lines at 184 and 253 nm and the line at 253 nm is absorbed by the LMCT band^[38] (Table S1) giving raise to the excited state of the porphyrin/corrole, prone to reduction of the metal center. The absorptivities of the LMCT bands diminish in the following order: NO_2^- (28.8, 267) > Cl_2^- (15.7, 291) > TP (12.2, 264). Similarly, the TON and TOF values of hydrogen production catalyzed by the cobalt corroles descend in the order (TON, TOF in min^{-1}): $-\text{NO}_2$ (76, 1.3) > TP- (30, 0.5) > $-\text{Cl}_2$ (28, 0.5). It would seem that the degree to which each cobalt corrole is able to absorb radiation from the lamp is correlated with its H_2 production capacity, but the differences in TOF and TON are not large.

It can be concluded that the substituents on the aromatic rings do not exert a major role on the efficiency of the catalyst, except in the modification of the absorptivities of the LMCT bands. This is possibly due to the fact that either with or without TP, the energy of the Hg lamp is so high that all studied systems are effectively reduced to Co^{I} or Fe^{I} .

A proposed mechanism for the catalytic reduction of water to hydrogen is presented in Scheme 2 which shows the formation of a hydride cobalt adduct which can be described as $\text{Co}^{\text{III}}\text{-H}$ or $\text{Co}^{\text{III}}\text{-H}^-$. The so formed cobalt hydride can be attacked by a proton to produce H_2 and re-form the catalyst [$\text{Co-Cor}^{\text{III}}$] in order to restart the catalytic cycle. This pathway is postulated as the main one, the difference being that when working with the sensitizer (TP), instead of Co^{III} Co^{II} is obtained, as described above (see equations 1-8).

By irradiation using a UV lamp, the reduced catalysts are obtained by electron donation from TEA; in some cases, these processes are $\text{M}^{\text{III}}\text{Corr} \rightarrow \text{M}^{\text{II}}\text{Corr}$, and in others $\text{M}^{\text{II}}\text{Corr} \rightarrow \text{M}^{\text{I}}\text{Corr}$. If $\text{M}^{\text{II}}\text{-Cor}$ is the main product, then the hydride can be formulated as $\text{H}^-\text{Co}^{\text{III}}\text{-Cor}$, which could dimerize and/or liberate H^- to produce H_2 .

This mechanism was previously proposed by Gross and coworkers, based on theoretical calculations.^[39]



Scheme 2. Proposed mechanism for the photocatalytic production of H_2 from water.

The relatively low TON values observed are probably due to bleaching of the catalyst by the UV light and/or hydrogenation of the macrocycle.

- *Co(III)-p-nitro phenyl corrole adsorbed on carbon nanotubes*

We have proved that it is possible to obtain hydrogen from water by reducing metallocorrole catalysts by UV irradiation and that in the presence and absence of TP, $\text{NO}_2\text{-Cor-Co}$ was the most effective catalyst. Therefore, we decided to adsorb the $\text{Co(III)-p-nitro phenyl corrole}$ on carbon nanotubes and study the catalytic performance of this nanocomposite.

The MWNT were activated^[27] and modified with $\text{Co(III)-p-nitro phenyl corrole}$ (MWNT/ $\text{NO}_2\text{-Cor-Co}$). The morphology

FULL PAPER

WILEY-VCH

and structure of the prepared nanocomposite were analyzed by TEM and SEM (Figure 3, S8 and S9).^[40] The general aspect of the uncoated and the functionalized nanotubes is similar in terms of diameter and length. However, the functionalized nanotubes present a thin layer of NO₂-Cor-Co, which is exclusively located around the nanotubes surface and is corroborated by a more intense contrast in the TEM images and the different aspect of the nanomaterial on the SEM micrograph.^[27,41] The amount of adsorbed corrole on the nanotubes was determined to be (0.06 ± 0.02)% of the total weight of the nanocomposite.

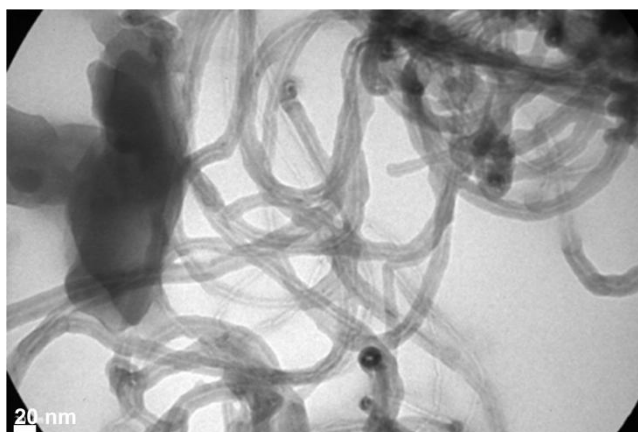


Figure 3. TEM image of MWNT/NO₂-Cor-Co. The corrole coating can be observed as a shade when the image is compared with the TEM image of unmodified MWNTs (Figure S8).

The UV-vis signals of corroles adsorbed on the nanotube surface are considerably broadened and red-shifted (~12 nm), clearly indicating the formation of conjugated corrole-MWNT with a strong π - π interaction (Figure S10).^[40,42–44] Moreover, after sonication, the absorbance spectra of MWNT solutions show a maximum at 264 nm^[45–47] which is also red-shifted (~30 nm) after the modification. The shift observed is a direct evidence of the π - π interaction between the nanotube sidewall and the corrole ring in the nanocomposite dispersion.^[48] The Resonant Raman (RR) features observed in the spectra given for NO₂-Cor-Co mainly arise from pyrrole and phenyl units of the macrocycle (Figure 4 and Table S2).^[49–51] It is worth mentioning that in the nanocomposites some small signals in the low frequency region (380, 990, 1074 and 1234 cm⁻¹) corresponding to the corrole molecule can be observed.

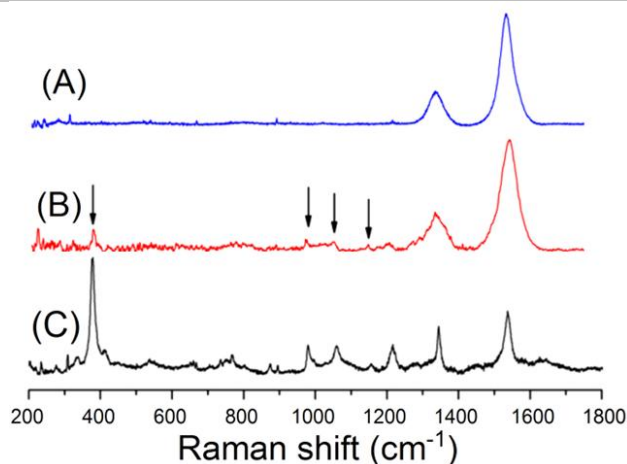


Figure 4. Raman Spectra of MWNT (A), (B) MWNT/NO₂-Cor-Co and (C) Co-corrole (normalized). Black arrows indicate the signals due to the immobilized corrole.

On the other hand, the characteristic Raman spectrum of MWNT in the range of 200–1800 cm⁻¹ is dominated by two peaks: one at 1371 cm⁻¹ and another one at 1577 cm⁻¹,^[52–54] which downshifts (6 cm⁻¹) in the nanocomposite, suggesting non-covalent strong interactions, such as hydrogen bonds and π - π stacking between the corrole ring and MWNT.^[55]

The photocatalytic performance of the nanocomposite was studied by UV-Vis spectroscopy. Figure S11 depicts the temporary changes of the Soret band while irradiating. These results also evidenced in the transition Co^{III}→Co^{II}→Co^I, proving that there is also a direct effect of the irradiation on the reduction of the metal center of the corroles present in the nanocomposites.

Hydrogen production by photocatalysis was confirmed by measuring the gas volume with a burette and also by quantifying H₂ through GC-TCD analysis of the H₂ peak (Table 3). Figure 5 shows the volume of H₂ produced vs time measured by the gas burette using MWNT/NO₂-Cor-Co. TON and TOF values for these experiments are shown in Table 3. It is worth mentioning that no gas is produced unless water is added. Experiments were performed with MWNT without metallocorrole, in which no hydrogen is obtained; this shows that the MWNT/NO₂-Cor-Co catalyst is that it produces hydrogen in the presence of water.

Table 3. Photocatalytic parameters obtained for hydrogen production by using MWNT/NO₂-Cor-Co.

Exp.	Gas burette		GC-TCD	
	dioxane ^[a]	buffer ^[b]	dioxane ^[a]	buffer ^[b]
Solvent				
TON×10 ⁵	5.11±1.26	7.01±1.23	4.20±1.03	7.01±1.09
TOF (min ⁻¹) ×10 ⁴	0.84±0.08	1.20±0.10	0.72±0.09	1.20±0.02

^[a] All experiments were performed in triplicate. The reactions were carried out at r.t and with continuous UV irradiation in 1,4-dioxane.

^[b] All experiments were performed in triplicate. The reactions were carried out at r.t and with continuous UV irradiation. 7.5×10⁻⁶ mol of catalyst in buffer formate.

FULL PAPER

WILEY-VCH

Considering the above results we proceeded to study MWNT-NO₂-Cor-Co toward H₂ production at pH = 3 (formate buffer). A larger amount of H₂ was obtained, since a higher concentration of H⁺ is present.^[39]

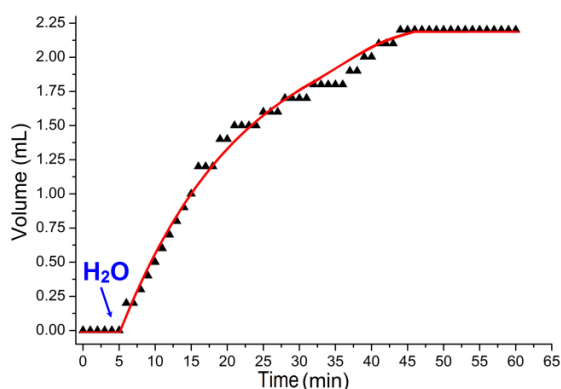


Figure 5. H₂-production using MWNT-NO₂-Cor-Co in buffer formate pH = 3, with the setup shown in Figure S1.

The catalytic parameters obtained for the nanocomposites are several orders of magnitude higher than those obtained with the corroles in solution. Furthermore, the TON value is very similar to that obtained electrochemically with the use of metallocorroles by Gross and collaborators ($>10^7$), although the TOF value is several orders of magnitude higher in our case (10^4 versus 10), and the pH much less acidic (pH = 0.3 vs. pH = 3).^[39]

MWNTs are good electron acceptors and act as effective electron transfer units because of their high electrical conductivity and high electron storage capacity.^[56,57] Therefore, in the current system the MWNT act as a photo-activated electron acceptor and electron-storage system that promotes interfacial electron transfer processes towards the deposited metallocorroles, increasing enormously the reduction rate of the metal center.^[23,58] Moreover, the presence of the nanotubes in the nanocomposite can inhibit the recombination of photo-generated electrons, improving the photocatalytic activity.^[23,59]

The transmission stability of promoted electrons between the nanotubes and the conduction band is enhanced by the strong π - π interaction and intimate contact between the corrole ring and the surface of the nanotubes, which was corroborated by UV-Vis and Raman analysis.

The nanocomposites were also studied by CV (Figure S12), the voltammograms show two irreversible processes, and a reversible one: an oxidation process (III), due to the Co^{IV}/Co^{III} couple and two reduction processes, irreversible I (MWNT) and reversible II (probably Co^{III}/Co^{II}), respectively, indicating the presence of the metallocorrole. In order to

study the photoelectrochemical performance of the nanocomposite, CVs between -1000 to +200 mV were recorded while irradiating (Figure 6A). Without irradiation, a reversible wave at -526 mV vs. NHE of about $\sim 3\mu\text{A}$ was observed, which probably corresponds to the redox couple Co^{III}/Co^{II}. But after 20 min of irradiation, an increase in the amplitude ($\sim 8\mu\text{A}$) and a shift of the peak to a less negative reduction potential (-251 mV) was detected. Not only is it possible to reduce the overpotential by almost 300 mV by irradiation, also the current -and therefore the reduction rate- is tripled.

So, photoamperometric measurements were performed at -251 mV. The response of the current to the addition of water is shown in Figure 6B. The negative current increases with the amount of added water, with the consequent appearance of H₂ bubbles. The volume of gas produced was measured by a gas burette, and 1.2 mmol of H₂ were obtained by adding 27 mmol of water, with TON and TOF values of $(1.0\pm 0.3)\times 10^7$ and $(3.4\pm 0.1)\times 10^5$, respectively. Id est, one order of magnitude higher compared to the values displayed in Table 4. After 30 minutes the catalyst was degraded.

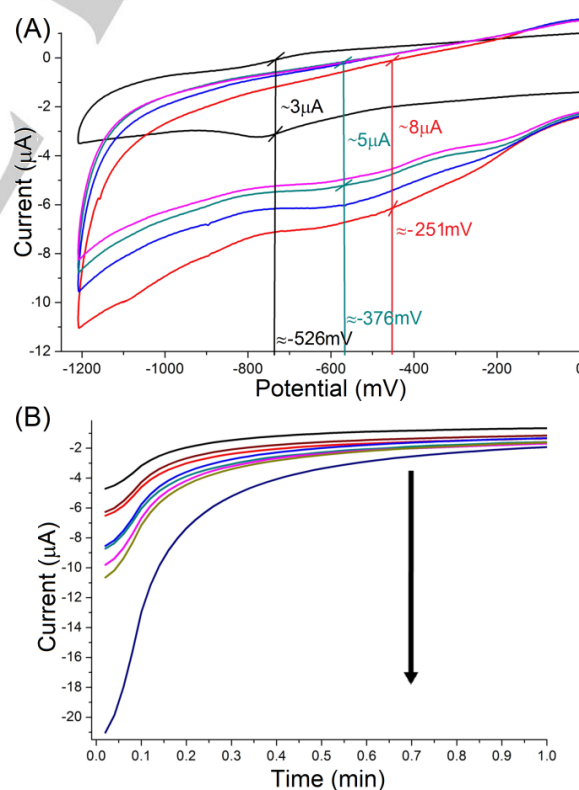


Figure 6. (A) CV vs. NHE, of the MWNT/NO₂-Cor-Co (5.8×10^{-8} M) in formate buffer, pH = 3, (scan rate = 100 mV/s) while irradiating: 0 min (black), 5 min (green), 15 min (blue), 20 min (red) and 30 min (pink). Full scan range [-1200 to 1000 mV]. (B) Photoelectrochemical amperometric measurements at -251 mV vs. NHE with addition of 0, 100, 200, 300, 400 and 500 μL of water. Total range 4800 s (see Figure S13).

The amount of gas produced by photoelectrocatalysis increases up to thirty times (Table 4) compared to the amount obtained by photocatalysis (Table 2). Therefore, photoelectrochemical catalysis accelerates the flow of electrons and the catalyst metal center is reduced faster and easier, obtaining larger amounts of gas at higher rates. It is worth mentioning that in this experiment an intense bubbling was observed.

Table 4. Catalytic parameters obtained in photoelectrocatalysis and electrocatalysis experiments. (Figure S14 shows the curve for dioxane experiments)

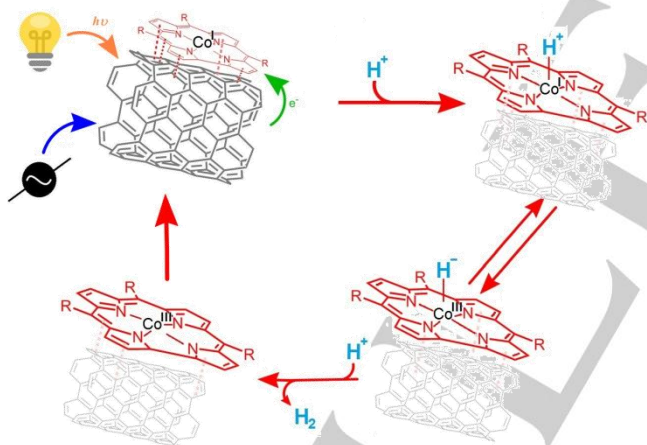
Exp.	Photoelectrocatalysis		Electrocatalysis	Photocatalysis
Catalyst	MWNT/NO ₂ -Cor-Co		Co-F ₈ ^[6]	Cobalaximes ^[6]
Solvent	dioxane	buffer	0.5 M H ₂ SO ₄	CH ₃ CN/H ₂ O (24:1) v/v
TON	(8.05±1.62)×10 ⁶	(1.01±0.33)×10 ⁷	>>10 ⁷	2.15×10 ³
TOF (min ⁻¹)	(2.68±12)×10 ⁵	(3.35±0.1)×10 ⁵	10	3.6
Potential (mV) ^[a]	-251	-251	-241	-886

^[a] Measured potentials vs. NHE.

^[b] Reference^[39].

^[c] Reference^[60].

A proposed mechanism for the photoelectrocatalytic reduction of water to hydrogen is presented in Scheme 3 which shows the formation of a hydride cobalt adduct which can be described as Co^(III)-H or Co^(III)-H⁻. The formed cobalt hydride can be attacked by a proton to produce H₂ and reform the catalyst [Co-Cor^(III)] in order to restart the catalytic cycle.



Scheme 3. Proposed mechanism for the photoelectrocatalytic production of H₂ from water.

Conclusions

It is possible to obtain hydrogen from water by reducing metalcorrole catalysts by UV irradiation; in some cases, M^{III}Cor→M^{II}Cor processes occur, and in others, M^{II}Cor→M^ICor.

In the presence and in the absence of TP, NO₂-Cor-Co resulted to be the most efficient catalyst, probably due to the electron-withdrawing effect of the -NO₂ substituent. However,

the differences in TON and TOF are not significant for different substituents on the aromatic rings. Therefore, we conclude that they do not exert a major role on the efficiency of the catalyst, although they do affect the reduction potential of the Co(II)/Co(I) redox couple.

Spectroscopic data suggest that Co(I) and/or Co(II) is the active form of catalyst that generates hydrogen, which was also demonstrated by Gross and coworkers.^[39] The difference in catalytic efficiency between cobalt and iron follows the pattern shown by the ring substituents and is also small.

Other catalysts that have similar structures with cobalt as metal center have shown production of hydrogen with a TON and TOF a little lower and much more severe reaction conditions than those used in this work.^[61]

Possibly, most metallocorroles could show photocatalytic activity for the production of hydrogen from water, regardless of the substituents or the metal center. Although the obtained photocatalytic activity in solution is relatively low, it can be enormously increased by immobilizing the catalysts on surfaces. This was shown by adsorbing Co(III)-p-nitro phenyl corrole on carbon nanotubes and studying the catalytic performance of this nanocomposite

The metallocorroles adsorbed on nanotubes showed a spectacular catalytic response. It is possible to reduce the overpotential to very low values (-251 mV vs. NHE) with a huge catalytic efficiency for hydrogen production. It can be said that the results achieved so far are innovative and powerful, since through the photoelectrochemical process it was possible to obtain 1 mmol of H₂ by using a minuscule amount of catalyst, in the order of picograms.

It is important to remember that the best catalyst should present high TON and TOF values and low over potentials. So MWNT-NO₂-Cor-Co, which is comparable to that developed by Gross,^[39] shows a similar overpotential, similar TON values, but much higher TOF values. Moreover: our catalyst works at pH = 3, while Gross's catalysts was tested in 0.5 M H₂SO₄ (pH = 0.3). With the data collected in this work and other recent publications, we can construct a graph evaluating the catalytic parameters, shown in Figure 7, adding the best molecular catalysts that we were able to find in the literature,^[17,39] compared to the one developed in this work.

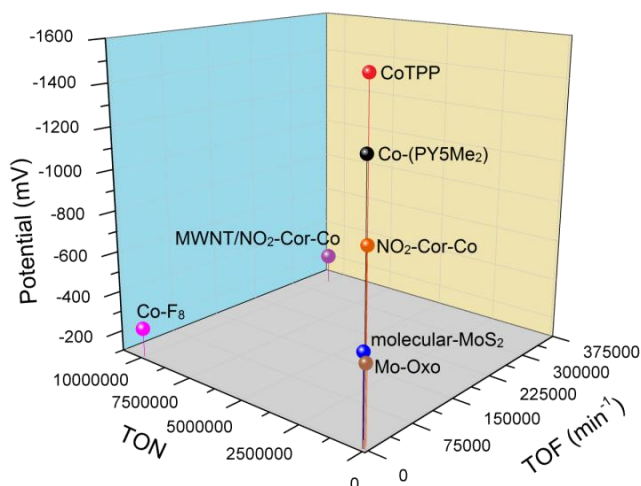


Figure 7. Plot of the catalytic parameters obtained from the literature and from Tables 1. Potential reported vs. NHE. Violet (MWNT/NO₂-Cor-Co), red (CoTPP), orange (NO₂-Cor-Co), pink^[39], black^[62], blue^[63] and brown^[64].

The best catalyst in the plot would be the one located on the vertex (highest TON and TOF value, lowest overpotential).

The immobilization approach without linkers reported in this work provides a simple and efficient methodology for the future study of the activity and stability of a variety of molecular catalysts in aqueous media. Furthermore, the photoelectrochemical catalytic efficiency increased 5 orders of magnitude when adsorbing the molecular catalysts onto carbon nanotubes.

Experimental Section

- Chemicals

Triethylamine (TEA), *p*-terphenyl (TP) and ferrocene (Fc), substituted benzaldehydes (*p*-nitrobenzaldehyde, 2,6-dichlorobenzaldehyde and benzaldehyde), pyrrole, were purchased from Sigma-Aldrich. N(Bu)₄PF₆ and KNO₃ were purchased from Merck.

Multiwalled carbon nanotubes (MWNT) (diameter 15±5 nm; length 1–5 μm) were purchased from Nano-Lab and were used without further purification.

Acetonitrile (MeCN), dichloromethane (DCM), 1,4-dioxane, and other organic solvents used were spectroscopic grade. These solvents were distilled from appropriate drying agents (CaH₂ and CaCl₂) under argon just prior to use. The water used in catalysis is grade Milli-Q.

- Instruments

All electrochemical measurements were performed with a TEQ 03 potentiostat, with a standard 3-electrode set up. For cyclic

voltammeteries (CV), the organic solvents used were dichloromethane (DCM) and acetonitrile (MeCN). Two platinum Pt-wire was used as reference and counter electrode and a 3 mm glassy carbon disc was used as a working electrode. N(Bu)₄PF₆ (0.1M) was used as supporting electrolyte. The solutions were free of air and voltammeteries were performed under an argon inert atmosphere. The pseudo-reference potential was calibrated with Fc and then transformed to E vs. SCE $E_{(SCE)} = E_{(Fc)} + 320$ mV. ¹H NMR spectra were performed on a Bruker AM-500 MHz in deuterated solvents obtained from Sigma-Aldrich (CDCl₃ and Pyridine-*d*₅).

A mercury lamp (Hg) of low pressure was used for irradiation. This lamp shows intense UV lines at 184 and 253 nm. The lamp was located at 40 cm (this distance was sufficient to prevent heating of the solution) of the quartz vessel for the experiments (a round-bottomed flask of 25 mL). The volume (mL) of the gas obtained from photocatalysis was quantified using a gas burette which is depicted in Figure S1. All volumes reported in this paper were measured at atmospheric pressure.

Mass spectrometry was accomplished for the detection of the gas products, using a Pfeiffer vacuum Omnistar GSD 320 gas analysis system with a quadrupole mass spectrometer QGM 220 (mass range 1–200 amu, PrismaPlus) with ion gas tight ion source, iridium-filament with secondary electron multiplier C-SEM and Faraday detectors. QUADERA software was used for data acquisition and control. The setup involves placing the gas analyzer capillary at one of the outputs of a booth-necked quartz flask containing solution of the metallocorrole. The output was free to perform water additions, using a micro syringe, through a septum closure. The gas detector was connected to the photocatalytic system as shown in Figure S4.

The UV-visible spectra were obtained using an Agilent 8453 diode array spectrophotometer, with thermostatic bath and quartz cuvettes of 1 cm optical path. For sensitive measurements, Schlenk cuvettes and cuvettes with Teflon or silicone septa were used, allowing the addition of reagents by the use of syringes. In order to measure the UV-Vis spectra during the photocatalysis, the system shown in Figure S3 was designed and developed.

Nanotubes size and morphology were verified by TEM. MWNT and nanocomposites dispersed in acetonitrile were imaged in a TEM Zeiss EM109T Transmission Electron Microscope after placing drops of dispersion onto gold grids, 400 mesh (SPI, PA, USA), and allowing the liquid to dry in air at room temperature. The scanning electron micrographs were obtained using a Carl Zeiss NTS SUPRA 40 SEM with Field Emission Gun (FEG), operated at 3 kV.

Raman scattering spectra were collected on a Horiba Jobin Yvon Dilor XY 800 confocal microspectrometer, equipped with a CCD detector of 1024×256 pixels, a holographic grating of 2400 groves/mm and a 50-mW Ar laser (413 nm wavelength) as excitation source. Spectra were measured in the 100–1600 cm⁻¹ Raman shift

region, at 1 cm^{-1} spectral resolution. Measurements were carried out in conditions of high confocality (3 pixels of the CCD detector and $20\text{ }\mu\text{m}$ slit width) through a $100\times$ Leica metallurgical objective (numerical aperture of 0.9), which limits the diameter of the laser beam to about $1\text{ }\mu\text{m}$. All spectra were baseline corrected.

- *Metalloporphyrin and metalloporphyrin synthesis*

Corroles: tris-phenyl-Corrole (TP-Cor); and tris-(2,6-dichloro-phenyl)-Corrole, (Cl_2 -Cor) were synthesized by the method described by Gryko et al.^[14] While tris-(*p*-NO₂-phenyl)-Corrole, (NO₂-Cor) was prepared following the procedure by Paolesse et al.^[65] To diminish oxidative degradation of the corroles^[65,66], purification was performed by protecting chromatographic columns from light, and the products were stored under inert atmosphere. The purification step with silica gel column ($63\text{-}200\text{ }\mu\text{m}$ and $70\text{-}230$ mesh) was optimized, and the eluents used were: CHCl_3 for TP-Cor; CH_2Cl_2 : n-hexane (1:2) for Cl_2 -Cor; and CH_2Cl_2 for NO₂-Cor. The main spectroscopic and electrochemical parameters of the obtained ligands are summarized in Table S3.

Cobalt-corroles: To obtain the cobalt complexes, the synthetic route described by Guillard et al.^[67] was used. Cobalt (II) acetate tetrahydrate and corrole-were mixed in a 3:1 ratio and refluxed in a mixture of chloroform/methanol (7:3) for 90 min. The reaction was followed by UV-Vis. The obtained metalloporphyrins were purified with a basic alumina column using DCM as eluent. The main spectroscopic and electrochemical parameters of the obtained metallocomplexes are summarized in Table S1.

Iron-corroles: These complexes were obtained by using the technique described by Walker et al.^[68] Iron (II) chloride and the corroles were mixed in 5:1 ratio and refluxed in dimethylformamide (DMF) under inert atmosphere for 45 min. The reaction was followed by UV-Vis. The purification was carried out performing an acid-base extraction, and the organic fraction was then filtered through a short column of neutral alumina. The elution solvent differed depending on the metalloporphyrin: for TP-Cor-Fe, CHCl_3 was used and for Cl_2 -Cor-Fe and NO₂-Cor-Fe, pure DCM was used. The main spectroscopic and electrochemical parameters of the obtained metallocomplexes are summarized in Table S1.

- *Preparation of MWNT-corrole nanocomposites*

MWNT (10 mg) were sonicated in nitric acid (35 vol %) (25 mL) with a sonic bath (120 W max) (100% for 5 min and then 40% for 15 min) and then heated at 60°C for 12 h. The suspension was then cooled; vacuum filtered and washed with water. The nanotubes were redispersed in NaOH 2 M (100 mL) using the sonic bath (100% for 10 min) and then filtered and washed with deionized water, and then HCl 1 M followed by deionized water until the filtrate was neutral. Secondly, the MWNT were centrifuged and redispersed by sonication in the corrole chloroformic solution. After 12 h the MWNT-corrole nanocomposite was separated by centrifugation and washed

with chloroform to remove the molecules of corrole not adsorbed on the nanotube surface.

- *Determination of the amount of adsorbed corroles on the nanotubes*

The amount of adsorbed corroles on the nanotubes surface was measured by un-adsorbing and separating the corroles from the nanotubes using a column of neutral alumina. Then, the obtained corrole solution was evaporated and the solid was dissolved in 2.5 mL of DCM. The concentration was calculated by measuring the absorbance of this solution at 422 nm and using the Lambert-Beer law: $A = \epsilon \cdot l \cdot [C]$. Where: $\epsilon = 98.2 \times 10^3\text{ M/cm}$; $l = 1\text{ cm}$; and $[C]$ = corrole molar concentration. The procedure was repeated three times for each nanocomposite and the average value was expressed

The calculated $[C]$ was $4.73 \times 10^{-6}\text{ M}$. So, for a volume of 2.5 mL the amount of corrole was $(1.22 \pm 0.13) \times 10^{-10}\text{ mol}$. This calculation was done in triplicate and the reproducibility was checked. The mass of NO₂-Cor-Co calculated was $(0.84 \pm 0.21)\text{ }\mu\text{g}$, representing, approximately the $(0.06 \pm 0.02)\%$ of the total weight of the nanocomposite initial mass $(1.4 \pm 0.1)\text{ mg}$.

- *Photocatalytic and Photoelectrocatalytic experiments*

Photocatalytic experiments were done with a medium pressure mercury (Hg) lamp. The light emitted is bluish-white color, contains no red radiation. Mercury lamps have various emission lines in both the visible and UV with considerable intensity. For this work the line is located at 253 nm excites the LMCT band of the corroles, located at ca. 200-250 nm.

Photoelectrocatalytic experiments were performed combining amperometry at -450 mV vs. Ag^0/AgCl with irradiation by the Hg lamp. Two conditions were studied: a) deoxygenated 1,4-dioxane solutions containing TEA (5 vol %) and TP ($3\text{ mmol}\cdot\text{L}^{-1}$); and b) formate buffer pH 3, 0.1 M. Blanks in all cases (with no catalyst) were performed and no gas formation was observed. Experiments were performed in triplicate. Amount of catalyst used: $1.2 \times 10^{-10}\text{ mol}$.

Blank experiments performed with no catalyst-gas production was not observed. Evolved H_2 volume measurements were performed using 7.5×10^{-6} moles of catalyst and 2 successive aliquots of 200 μL of water. No gas production was obtained with experiments performed with no UV light or with filters that did not allow the passage of wavelength below 375 nm.

- *Measurements of H_2 production*

A Shimadzu-14A gas chromatograph with Thermal conductivity detector (TCD) was employed for the analytical quantification of H_2 . This was equipped with two packed columns of stainless steel, one internal and other external to the gas chromatograph. The output of the first column of 2 m long and 3 mm ID was connected to a channel of the detector. The second column of 0.5 m long and 3 mm ID, connected in series, was submerged in a bath of ethanol-liquid

nitrogen mix. The output was connected to the reference channel of the detector, previously passing through the oven to take the same temperature. Both columns were filled with Molecular Sieve 13X. The columns operating temperatures were 110 °C for the internal and -100 °C for the external column. The detector temperature was 110 °C. As gas carrier, nitrogen chromatographic quality was used, at a pressure of 2 kg/cm² at the head of the column. The system for the introduction of sample consisted of a 6-way valve with a loop of 1 mL (Valco Instrument Co. Inc.) attached to a glass manometer of Hg of two branches. The entire system was connected, through a needle valve, to a vacuum pump made for LEYBOLD GmbH (model MINI A) working at room temperature of 24 °C. This system allows the transfer the gas sample in a container of fixed volume to the loop, and the introduction to the chromatograph. Successive injections at different pressures, allows the replicated of same sample. For the acquisition interface from Data Apex Co. (model U-PAD2 USB) was used with Clarity Lite Software for data analysis. Figure S2 shows the experimental setup for this step. Amount of catalyst used: 1.2×10⁻⁹ mol.

The gas (H₂) production was determined by connecting the reaction cell with a gas burette (25.0 ± 0.5 mL), which's lower end is connected by a hose to an ampoule and all system is sealed with Hg⁰. All volumes reported in this paper were taken at atmospheric pressure as the internal pressure is equalized with the outside. Figure S1 shows the experimental setup for this step. Amount of catalyst used: 1.2×10⁻¹⁰ mol.

Acknowledgements

This work was financially supported by CONICET (PIP 112 201001 00125). MAMV and AYT thank CONICET for a fellowship grant. NIN, MH, EJC and FD are members of CONICET.

Keywords: photocatalysis; electrocatalysis; metallocorroles; hydrogen; synthesis; water splitting.

- [1] K. Peuntinger, T. Lazarides, D. Dafnomili, G. Charalambidis, G. Landrou, A. Kahnt, R. P. Sabatini, D. W. McCamant, D. T. Gryko, A. G. Coutsolelos, et al., *J. Phys. Chem. C* **2013**, *117*, 1647–1655.
- [2] H.-Y. Liu, M. H. Mahmood, S.-X. (Samuel) Qiu, C. K. Chang, *Coord. Chem. Rev.* **2013**, *257*, 1306–1333.
- [3] D. T. Gryko, J. P. Fox, D. P. Goldberg, *J. Porphy. Phthalocyanines* **2004**, *8*, 1091–1105.
- [4] E. Vogel, S. Will, A. S. Tilling, L. Neumann, J. Lex, E. Bill, A. X. Trautwein, K. Wieghardt, *Angew. Chemie Int. Ed. English* **1994**, *33*, 731–735.
- [5] S. Will, J. Lex, E. Vogel, H. Schmickler, J.-P. Gisselbrecht, C. Hauptmann, M. Bernard, M. Gorss, *Angew. Chemie Int. Ed. English* **1997**, *36*, 357–361.
- [6] Z. Gross, *JBIC J. Biol. Inorg. Chem.* **2001**, *6*, 733–738.
- [7] A. Mohammed, J. J. Weaver, H. B. Gray, M. Abdelas, Z. Gross, *Tetrahedron Lett.* **2003**, *44*, 2077–2079.
- [8] H. Park, C. D. Vecitis, W. Choi, O. Weres, M. R. Hoffmann, *J. Phys. Chem. C* **2008**, *112*, 885–889.
- [9] L. Shi, H.-Y. Liu, H. Shen, J. Hu, G.-L. Zhang, H. Wang, L.-N. Ji, C.-K. Chang, H.-F. Jiang, *J. Porphy. Phthalocyanines* **2009**, *13*, 1221–1226.
- [10] I. Aviv-Harel, Z. Gross, *Coord. Chem. Rev.* **2011**, *255*, 717–736.
- [11] Z. Gross, N. Galili, I. Saltsman, *Angew. Chemie Int. Ed.* **1999**, *38*, 1427–1429.
- [12] Z. Gross, N. Galili, L. Simkhovich, I. Saltsman, M. Botoshansky, D. Bläser, R. Boese, I. Goldberg, *Org. Lett.* **1999**, *1*, 599–602.
- [13] R. Paolesse, S. Mini, F. Sagone, T. Boschi, L. Jaquinod, D. J. Nurco, K. M. Smith, *Chem. Commun.* **1999**, 1307–1308.
- [14] D. T. Gryko, *Chem. Commun.* **2000**, 2243–2244.
- [15] D. T. Gryko, K. Jadach, *J. Org. Chem.* **2001**, *66*, 4267–4275.
- [16] R. M. Kellett, T. G. Spiro, *Inorg. Chem.* **1985**, *24*, 2373–2377.
- [17] M. A. Morales Vásquez, S. A. Suárez, F. Doctorovich, *Mater. Chem. Phys.* **2015**, *159*, 159–166.
- [18] R. K. Hocking, S. D. George, Z. Gross, F. A. Walker, K. O. Hodgson, B. Hedman, E. I. Solomon, *Inorg. Chem.* **2009**, *48*, 1678–1688.
- [19] F. M. Toma, A. Sartorel, M. Iurlo, M. Carraro, P. Parisse, C. Maccato, S. Rapino, B. R. Gonzalez, H. Amenitsch, T. Da Ros, et al., *Nat. Chem.* **2010**, *2*, 826–831.
- [20] F. Li, L. Li, L. Tong, Q. Daniel, M. Göthelid, L. Sun, *Chem. Commun.* **2014**, *50*, 13948–13951.
- [21] H. Li, B. Zhou, Y. Lin, L. Gu, W. Wang, K. A. S. Fernando, S. Kumar, L. F. Allard, Y.-P. Sun, *J. Am. Chem. Soc.* **2004**, *126*, 1014–1015.
- [22] G. Bottari, G. de la Torre, T. Torres, *Acc. Chem. Res.* **2015**, *48*, 900–910.
- [23] F. D'Souza, R. Chitta, A. S. D. Sandanayaka, N. K. Subbaiyan, L. D'Souza, Y. Araki, O. Ito, *J. Am. Chem. Soc.* **2007**, *129*, 15865–15871.
- [24] D. M. Guldi, G. M. A. Rahman, F. Zerbetto, M. Prato, *Acc. Chem. Res.* **2005**, *38*, 871–878.
- [25] Y. Tachibana, L. Vayssieres, J. R. Durrant, *Nat. Photonics* **2012**, *6*, 511–518.
- [26] Y. Cheng, A. Memar, M. Saunders, J. Pan, C. Liu, J. D. Gale, R. Demichelis, P. K. Shen, S. P. Jiang, *J. Mater. Chem. A* **2016**, *4*, 2473–2483.
- [27] I. Hijazi, T. Bourgeteau, R. Cornut, A. Morozan, A. Filoramo, J. Leroy, V. Derycke, B. Jousseme, S. Campidelli, *J. Am. Chem. Soc.* **2014**, *136*, 6348–6354.
- [28] Q. Zhong, V. V. Diev, S. T. Roberts, P. D. Antunez, R. L. Brutchey, S. E. Bradforth, M. E. Thompson, *ACS Nano* **2013**, *7*, 3466–3475.
- [29] A. Choi, H. Jeong, S. Kim, S. Jo, S. Jeon, *Electrochim. Acta* **2008**, *53*, 2579–2584.
- [30] W. Tu, J. Lei, H. Ju, *Electrochem. Commun.* **2008**, *10*, 766–769.
- [31] F. Li, B. Zhang, X. Li, Y. Jiang, L. Chen, Y. Li, L. Sun, *Angew. Chemie* **2011**, *123*, 12484–12487.
- [32] T. Dhanasekaran, J. Grodkowski, P. Neta, P. Hambright, E. Fujita, *J. Phys. Chem. A* **1999**, *103*, 7742–7748.
- [33] J. Grodkowski, P. Neta, E. Fujita, A. Mohammed, L. Simkhovich, Z. Gross, *J. Phys. Chem. A* **2002**, *106*, 4772–4778.
- [34] B. Ramdhanie, J. Telsler, A. Caneschi, L. N. Zakharov, A. L. Rheingold, D. P. Goldberg, *J. Am. Chem. Soc.* **2004**, *126*, 2515–2525.
- [35] S. Matsuoka, T. Kohzaki, C. Pac, A. Ishida, S. Takamuku, M. Kusaba, N. Nakashima, S. Yanagida, *J. Phys. Chem.* **1992**, *96*, 4437–4442.
- [36] D. Behar, T. Dhanasekaran, P. Neta, C. M. Hosten, D. Ejeh, P. Hambright, E. Fujita, *J. Phys. Chem. A* **1998**, *102*, 2870–2877.
- [37] Z. Ou, A. Lü, D. Meng, S. Huang, Y. Fang, G. Lu, K. M. Kadish, *Inorg. Chem.* **2012**, *51*, 8890–8896.
- [38] D. N. Hendrickson, M. G. Kinnaird, K. S. Suslick, *J. Am. Chem. Soc.* **1987**, *109*, 1243–1244.
- [39] B. Mondal, K. Sengupta, A. Rana, A. Mohammed, M. Botoshansky, S. G. Dey, Z. Gross, A. Dey, *Inorg. Chem.* **2013**, *52*, 3381–3387.
- [40] Z. Wang, H. Lei, R. Cao, M. Zhang, *Electrochim. Acta* **2015**, *171*, 81–88.
- [41] J. Wang, Y. Chen, W. J. Blau, *J. Mater. Chem.* **2009**, *19*, 7425.
- [42] D. Baskaran, J. W. Mays, X. P. Zhang, M. S. Bratcher, *J. Am. Chem. Soc.* **2005**, *127*, 6916–6917.
- [43] G. A. M. Sáfar, H. B. Ribeiro, L. M. Malard, F. O. Plentz, C. Fantini, A. P. Santos, G. de Freitas-Silva, Y. M. Idemori,

- Chem. Phys. Lett.* **2008**, *462*, 109–111.
- [44] G. Magadur, J.-S. Lauret, V. Alain-Rizzo, C. Voisin, P. Roussignol, E. Deleporte, J. A. Delaire, *ChemPhysChem* **2008**, *9*, 1250–1253.
- [45] G. A. Rance, D. H. Marsh, R. J. Nicholas, A. N. Khlobystov, *Chem. Phys. Lett.* **2010**, *493*, 19–23.
- [46] J. Yu, N. Grossiord, C. E. Koning, J. Loos, *Carbon N. Y.* **2007**, *45*, 618–623.
- [47] A. G. Ryabenko, T. V. Dorofeeva, G. I. Zvereva, *Carbon N. Y.* **2004**, *42*, 1523–1535.
- [48] P. Huang, C. Xu, J. Lin, C. Wang, X. Wang, C. Zhang, X. Zhou, S. Guo, D. Cui, *Theranostics* **2011**, *1*, 240–250.
- [49] E. Steene, T. Wondimagegn, A. Ghosh, *J. Inorg. Biochem.* **2002**, *88*, 113–118.
- [50] K. Lewandowska, B. Barszcz, J. Wolak, A. Graja, M. Grzybowski, D. T. Gryko, *Dye. Pigment.* **2013**, *96*, 249–255.
- [51] I. H. Wasbotten, T. Wondimagegn, A. Ghosh, *J. Am. Chem. Soc.* **2002**, *124*, 8104–8116.
- [52] T. Odedairo, J. Ma, Y. Gu, J. Chen, X. S. Zhao, Z. Zhu, *J. Mater. Chem. A* **2014**, *2*, 1418–1428.
- [53] I. Pócsik, M. Hundhausen, M. Koós, L. Ley, *J. Non. Cryst. Solids* **1998**, *227–230*, P, 1083–1086.
- [54] L. Bokobza, *Express Polym. Lett.* **2012**, *6*, 601–608.
- [55] V. A. Karachevtsev, E. S. Zarudnev, S. G. Stepanian, A. Y. Glamazda, M. V. Karachevtsev, L. Adamowicz, *J. Phys. Chem. C* **2010**, *114*, 16215–16222.
- [56] T. A. Saleh, V. K. Gupta, *J. Colloid Interface Sci.* **2011**, *362*, 337–344.
- [57] J. E. Riggs, Z. Guo, D. L. Carroll, Y.-P. Sun, *J. Am. Chem. Soc.* **2000**, *122*, 5879–5880.
- [58] D. M. Guldi, H. Taieb, G. M. A. Rahman, N. Tagmatarchis, M. Prato, *Adv. Mater.* **2005**, *17*, 871–875.
- [59] F. D'Souza, S. K. Das, M. E. Zandler, A. S. D. Sandanayaka, O. Ito, *J. Am. Chem. Soc.* **2011**, *133*, 19922–19930.
- [60] J. L. Dempsey, B. S. Brunschwig, J. R. Winkler, H. B. Gray, *Acc. Chem. Res.* **2009**, *42*, 1995–2004.
- [61] S. Losse, J. G. Vos, S. Rau, *Coord. Chem. Rev.* **2010**, *254*, 2492–2504.
- [62] Y. Sun, J. P. Bigi, N. A. Piro, M. L. Tang, J. R. Long, C. J. Chang, *J. Am. Chem. Soc.* **2011**, *133*, 9212–9215.
- [63] H. I. Karunadasa, E. Montalvo, Y. Sun, M. Majda, J. R. Long, C. J. Chang, *Science (80-.)* **2012**, *335*, 698–702.
- [64] H. I. Karunadasa, C. J. Chang, J. R. Long, *Nature* **2010**, *464*, 1329–1333.
- [65] R. Paolesse, S. Nardis, F. Sagone, R. G. Khoury, *J. Org. Chem.* **2001**, *66*, 550–556.
- [66] J. Wojaczyński, M. Duszak, L. Latos-Grażyński, *Tetrahedron* **2013**, *69*, 10445–10449.
- [67] J.-M. Barbe, G. Canard, S. Brandes, F. Jerome, G. Dubois, R. Guilard, *Dalt. Trans.* **2004**, 1208–1214.
- [68] F. A. Walker, S. Licoccia, R. Paolesse, *J. Inorg. Biochem.* **2006**, *100*, 810–837.

FULL PAPER

Text for Table of Contents:

Abstract

Introduction

Result and discussion

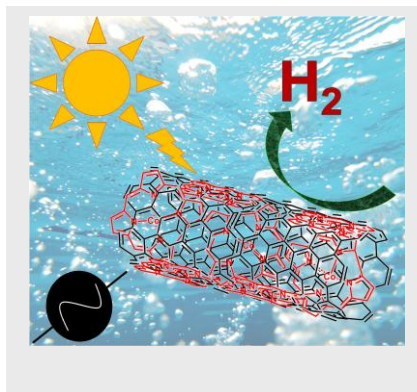
Conclusions

Experimental section

Acknowledgements

Keywords

References



Key Topic: Catalysis

*Miguel A. Morales Vásquez, Mariana Hamer, Nicolás I. Neuman, Alvaro Y. Tesio, Andrés Hunt, Horacio Bogo, Ernesto J. Calvo and Fabio Doctorovich**

Page No. – Page No.

Title:
Iron and cobalt corroles in solution and on carbon nanotubes as molecular photocatalysts for hydrogen production by water reduction

WILEY-VCH

Accepted Manuscript